Decay of neutron-deficient ^{103}In and ^{103}Cd isotopes

G. Lhersonneau, G. Dumont, K. Cornelis,[*] M. Huyse, and J. Verplancke

University of Leuven, Instituut voor Kern-en Stralingsfysika, Celestijnenlaan 200 D, B-3030 Leuven, Belgium
(Received 30 May 1978)

The decays of neutron-deficient ^{103}In and ^{103}Cd have been investigated. Sources were produced by (^{14}N,yp-xn) reactions on a natural Mo target. Singles spectra and various coincidence spectra involving γ rays, x rays, positrons, and conversion electrons have been performed on mass separated samples. The newly discovered activity ^{103}In ($T_{1/2} = 1.08 \pm 0.11$ min) was found to populate mainly the 7/2$^+$ excited ^{103}Cd state at 188 keV. About 200 lines were attributed to the 7.3 min ^{103}Cd decay. Coincidence relationships are given. A level scheme of ^{103}Ag is proposed.

RADIOACTIVITY ^{103}In, ^{103}Cd from Mo (^{14}N, yp xn) measured E_γ, I_γ, $\gamma\gamma$ coin, E_β ^{103}Cd and ^{103}Ag deduced levels α_k, J, π natural target, mass separation Ge (Li), Si (Li) detectors.

I. INTRODUCTION

The nuclides near the proton shell closure at $Z = 50$ (tin isotopes) have been intensively studied for a number of reasons. These reasons include studying neutron-neutron interactions when there are only a small number of protons present and studying the interaction of small numbers of protons (particle or holes) with a relatively simple core. At masses 100 and 132 the neutron shell closure leads to possible magic nuclei, of which ^{100}Sn remains undiscovered.

The investigation of the 103 mass chain was undertaken with the aim of identifying unknown nuclides near $N = Z = 50$ and observing more details of the level structure of known isotopes. The isotopes of In ($Z = 49$), Cd ($Z = 48$), and Ag ($Z = 47$) have been extensively studied down to $A = 104$. However, little is known about the mass chain 103. There existed no information on the ^{103}Cd levels either from the decay study of ^{103}In, or from in-beam experiments. The activity ^{103}In was not observed, while decay studies of ^{103}Cd showed contradictory results.[1,2] The ^{103}Ag isomeric ($T_{1/2} = 5$ s) and ground state ($T_{1/2} = 66$ min) decays have been previously studied.[1,5,6] Further decays to the stability valley are not expected to contribute significantly in our experiments because of their longer half-life. In this paper we report on the discovery of ^{103}In activity and the identification of more than 200 lines in the decay of ^{103}Cd and place 196 γ rays in a proposed level scheme of ^{103}Ag involving 60 levels.

II. EXPERIMENTAL PROCEDURE

The radioactive nuclides ^{103}In, ^{103}Cd, and ^{103}Ag were produced at the Louvain isotope separator on line (LISOL) facility described previously.[7]

The natural Mo filament of the separator ion-source was irradiated with a 72 MeV, ^{14}N^{3+} beam from the CYCLONE cyclotron at Louvain-la-Neuve. After diffusion out of the catcher, the reaction products were ionized and mass separated. The reactions of interest for producing ^{103}In and ^{103}Cd isotopes are mainly ^{92}Mo(N, $3n$)^{103}In and ^{92}Mo(N,$p2n$)^{103}Cd. The expected thick target yields were computed with the ALICE code.[8] The evaporation calculation was performed over all the partial waves for n, p, d, and α emission. The Myers and Swiatecky mass formulas were used without pairing corrections. For the other parameters default options as indicated in Ref. 9 were used. With the typical 2 μA current of the N^{3+} beam, about 7×10^5 and 9×10^6 particles/s for ^{103}In and ^{103}Cd, respectively, are expected. The experimental collection rate, under the same conditions, was estimated at 10^3 and 10^5 particles/s. The strong ^{103}Ag background (10^6 particles/s) is produced mostly (75%) by ^{92}Mo(N, $2pn$)^{103}Ag and ^{94}Mo(N, αn)^{103}Ag reactions rather than by ^{103}Cd decay, and arises in part from the high efficiency with which Ag passes through the isotope separator.

Single and coincidence γ spectra were taken with two Ge(Li) detectors with a resolution of 2.3 keV and a relative efficiency of 10% at the 1332.5 keV ^{60}Co line. The coincidence time resolution was about 20 ns, the chance coincidences were negligible. An intrinsic Ge x-ray detector of 400 eV resolution at the 59.5 keV ^{241}Am line was used in single and coincidence spectra for the study of low-energy γ rays. Conversion electron measurements were performed with a mini-orange spectrometer.[10]

The LISOL facility has two types of counting setups at its disposal. In the on-line mode, used for short half-lives, the separator beam is col-

lected on a movable aluminized Mylar tape. Spectra are taken both at a collection and at a remote decay station. In the off-line mode, the activity is implanted in a foil placed in the collector chamber of the separator. Moving the foil to the detectors usually takes less than 1 min. Owing to the longer half-life (7.3 min) and a better counting geometry, the ^{103}Cd decay studies are performed this way. For both modes typical activation and collection times are 2 to 3 times the half-life under investigation.

Studies of growth and decay have been used to determine the ^{103}In half-life. The 20 strongest transitions from ^{103}Cd have also been analyzed this way. However, the other transitions were assigned considering their occurrence in a simulated "pure" ^{103}Cd spectrum, and their absence in a simulated ^{103}Ag spectrum and natural background. The simulated pure spectra are obtained using the following procedure.

Assuming the natural background spectrum properly substracted and neglecting the weak and short living ^{103}In activity, the obtained spectra contain only counts from ^{103}Cd and ^{103}Ag decays. Using two independent spectra, S_1 and S_2, a pure spectrum of each of the component activities can be generated by a linear combination of the type $P = a_1 S_1 + a_2 S_2$. The coefficients are determined by the integration of peaks of known pure character. This method avoids the fitting of doublets with Cd and Ag components. The simulated spectra are analyzed in a conventional way, except that the count errors are now $(a_1^2 S_1 + a_2^2 S_2)^{1/2}$, that is, different from $\sqrt{P}$. The method has been tested on a simulated ^{103}Ag spectrum. Moreover, spectra of mass 104 have been recorded in order to deduce the x-ray patterns of the different elements. Disregarding them, only low energy γ rays remain present in the generated spectrum.

Three parameter (γ, γ, t) coincidences are recorded sequentially event by event on magnetic tape. The analysis is performed off-line with left- and right-side background windows set for every peak. The data are extracted using a matrix formalism.[11] The algorithm has been improved to provide an exact background subtraction for any choice of the side windows, under the assumption of a linear background. The increased freedom in choosing the windows proves to be of particular interest in the dense ^{103}Cd + ^{103}Ag spectrum. No correction for chance coincidences has been found necessary.

The Q_{EC} measurement of ^{103}Cd decay has been performed using a plastic scintillator telescope arrangement. Single spectra as well as β-γ coincidences were recorded. The positron branching to the ^{103}Ag ground state could not accurately be determined from the single β spectra due to the presence of the high background originating in ^{103}Ag decay. It was then deduced from the intensity of the annihilation peak in the generated pure ^{103}Cd γ spectra. A correction needed to be applied to the 511 keV intensity as the sources were not rigorously punctual for this radiation. It was estimated in order to reproduce the 511 keV intensity in the decay of ^{103}Ag, as deduced from the level scheme of Dietrich et al.[6]

III. EXPERIMENTAL RESULTS

A. ^{103}In

The multiscaled spectra of Fig. 1 show two lines of 187.93± 0.09(100) and 201.97± 0.12 keV (21± 3), decaying with a half-life of (1.08± 0.11) min. Owing to its intensity the 187.93 keV γ ray is expected to deexcite a level at the same energy, as shown in the partial decay scheme of Fig. 2.
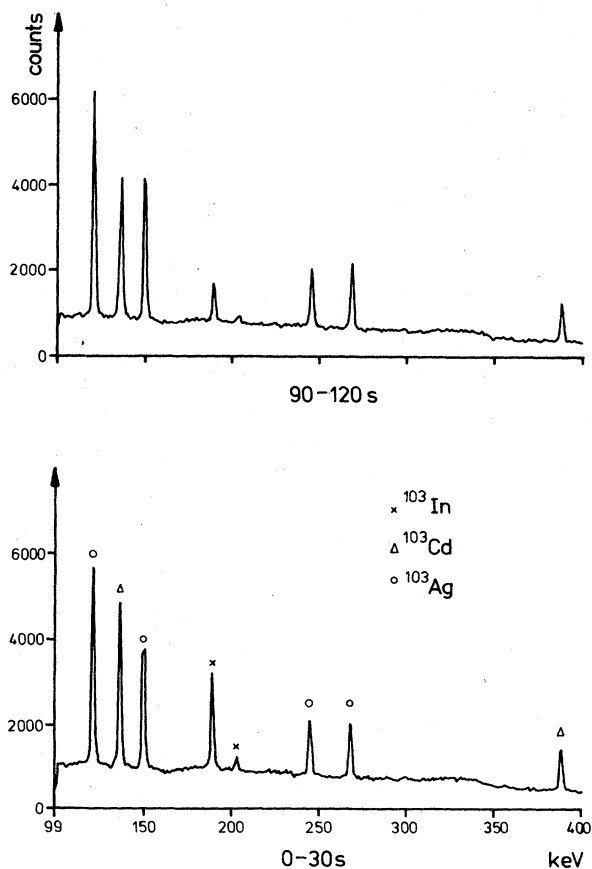

FIG. 1. Part of the multiscaled spectra showing the decay of the 188 keV and 202 keV lines attributed to the 1.1 min activity of ^{103}In.
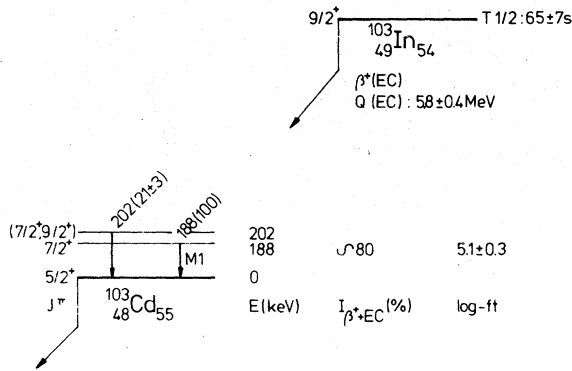
FIG. 2. Graphical summary of our results on the ^{103}In decay.

A second level at 202 keV is introduced as no 188–202 keV coincidence has been observed. The 188 keV line has also been observed by an in-beam study.[12] The conversion electron spectra were measured with the mini-orange spectrometer. The experimental α_K values of Table I attribute $M1$ character to the 188 keV transition and suggest even parity for the 202 keV level. Multiscaled β^+ spectra show counts above the β^+ end point energy of ^{103}Cd decay, decaying with the proper half-life. The deduced Q_{EC} value for ^{103}In decay of 5.8 ± 0.5 MeV agrees with most of the mass predictions[13,14] ranging from 5.2 MeV (Myers) to 6.4 MeV (Garvey). The deduced $\log ft$ values, using the Gove and Martin tables[15] are consistent with β^+ hindered allowed transitions. The systematics suggest $(\pi g_{9/2})^{-1}$ as the ^{103}In ground state, while the ^{103}Cd ground state is expected to be a $(\nu d_{5/2})$. The 188 keV level is assigned $J^\pi = \frac{7}{2}^+$ from its feeding by allowed decay from a $\frac{9}{2}^+$ state and its γ decay with a $M1$ component to the $\frac{5}{2}^+$ ^{103}Cd ground state. A unique assignment for the 202 keV level is difficult.

B. ^{103}Cd

The half-life (7.3 ± 0.1) min of ^{103}Cd has been determined previously.[1,2] There existed, however, no accord between the γ rays reported in these investigations. In our study about 200 lines are assigned to the ^{103}Cd activity. The transitions of

1080, 1448, and 1462 keV reported by Hansen et al.[1] are confirmed, but no evidence of the transitions from the other work[2] has been found. The isomeric $E3$ transition in ^{103}Ag of 134 keV previously studied[1,5] has also been observed. Table II lists the γ rays observed in single spectra, and those observed in coincidence spectra which are placed on the level scheme of Fig. 3. The γ rays observed in coincidence with the lines used as gate (marked with a dot at their upper end on the level scheme) are also listed. Most of the 60 levels are supported by coincidence data though with large statistical uncertainty in many cases (10^6 events of which about one-half are ^{103}Cd). However, a few high energy levels are supported by energy sum fitting and the absence of contradictory data. Table III lists the levels shown of Fig. 3.

IV. THE ^{103}Ag LEVEL SCHEME

The $\frac{7}{2}^+$ ground state and the $\frac{1}{2}^-$ isomeric state have been established previously.[16,5] A level is proposed at 27.56 keV and assigned $\frac{9}{2}^+$ spin and parity. The placement and assignment are supported by a number of pairs of γ rays with a 27 keV energy difference, coincidence evidence indicating that both γ rays with a 27 keV difference come from the same level, lack of coincidences between γ rays with the 27 keV difference, and the clear systematic presence of a low lying $\frac{9}{2}^+$ state.[17–23] Moreover, in the case of the 1448 keV γ ray, coincidences with the 27.56 keV γ ray were observed.

These three levels are used as a starting point to build the level scheme. A first group of levels at 1080, 1099, 1312, 1462, and 1476 keV is introduced on the basis of strong transitions at these energies, the occurrence of γ rays of the corresponding energies minus 27 keV, and the absence of coincidences between any of these γ rays. In the case of the 1080 and 1476 keV levels, strong evidence for placement of the 1052 (1080 to 27) and 1448 (1476 to 27) keV γ rays is found in the similarity of the coincidence spectra of the 27 keV energy difference pair members. Moreover, the 1476 keV level is supported by a 27–1448 keV coincidence. The 1284 (1312 to 27)

TABLE I. α_K of ^{103}In. Theoretical values have been taken from Ref. 25.

E (keV)	$E1$	$M1$	$E2$	Exp.
188	2.5×10^{-2}	7.7×10^{-2}	1.36×10^{-1}	$(6.5 \pm 1.1)10^{-2}$
202	2.1×10^{-2}	6.3×10^{-2}	1.05×10^{-1}	$(1.3 \pm .4)10^{-1}$

TABLE II. List of γ rays. P means this transition is shown on the level scheme Fig. 3. M means the peak is a multiplet resolved by coincidences, the components are listed below. C means coincident γ rays are indicated in front of the peaks on which gates were set. A transition in parentheses is considered as weakly coincident (relative intensity error > 0.3). A transition with a C is only observed in a coincidence spectrum. R means a level exists at the transition energy E_γ or $E_\gamma + 27$ or $E_\gamma + 134$ keV. D means there is a discrepancy between the energies from single and coincidence spectra, as no evidence is found for two different placements.

Energy		Intensity			Placement from/to	Coincidences observed in this gate and remarks
27.56	0.04	11.0	2.1		27/0	(1448)
69.37	0.06	0.67	0.11		590/521	
134.44	0.05	26.4	0.8		134/0	
188.3	0.6	0.3	0.2	C	2088/1901	1766
243.1	0.4	4.8	0.6		1705/1461	494, 511, 815, 1461 Ag peak at 243.96
264.4	0.6	1.1	0.3	C	1822/1557	
296.7	0.6	0.8	0.3	C	2199/1901	
318.0	0.8	0.2	0.1	C	2199/1880	
370.8	0.6	0.6	0.2	C	2199/1828	747, 1307, 1693
377.0	0.7	1.3	0.6	C	1476/1099	
386.97	0.07	30.2	0.8		521/134	(448), 511, 562, 688, (726), 736, (883), 940, 952, (1005), (1042), (1060), 1167, 1184, 1307, 1447, 1499, 1567, 1677, 1685, 1919, 1999, 2300, 2368. Weak evidence for a 2287/1901 387.2 (.8)
442.2	0.8	1.4	0.7	C	2401/1958	
456.34	0.07	24.4	0.6		590/134	494, 511, 620, (627), 654, 667, 717, (749), (766), 815, 871, 883, (1032), (1039), (1048), (1096), 1114, (1121), (1305), 1377, (1674), 2068, (2120), (2183), 2298
463.7	0.6	1.3	0.4	C	2020/1557	
477.12	0.20	2.0	0.3		1557/1080	1080
494.73	0.14	5.9	0.4	M		
494.3	0.4	4.4	2.0		2199/1705	243, 387, 456, 625, 1114, (1184), 1571
496.2	0.4	1.5	0.5		1958/1461	511, 1461
520.3	0.8	0.2	0.1	C	2401/1880	
526.69	0.32	1.0	0.2		(3188/2662)	Not shown, no clear coincidences
530.86	0.21	4.4	0.7	(M)		Ag peak at 531.92
					Not placed	(924)
532.1	0.4	3.8	0.5	C	2088/1557	(511), 1557
545.26	0.15	6.0	0.4	M		
544.4	0.4	3.0	0.8		2401/1856	563, 1856
546.4	0.4	3.0	0.8		1968/1422	1287
552.60	0.10	2.4	0.3		2521/1968	(546), 1461, 1834
562.93	0.07	15.0	0.5	M		
562.2	0.4	1.3	0.4		1083/521	387, 1005
563.0	0.4	7	3		590/27	721, 961, 1089, 1668
					Not assigned	544, 917, (1080), (1328), 1574
598.8	0.7	1.0	0.4	C	2020/1422	(1287)
620.09	0.16	3.0	0.3		1210/590	456, (741)
626.21	0.09	14.9	0.5	M		Ag peak at 625.9 keV
625.2	0.4	8.9	1.6		1705/1080	494, 511, (734), 815, 1052, 1080
627.0	0.4	6.0	1.1		2088/1461	(511), 1461
643.1	0.5	2.6	0.7	C	2199/1557	511, 1557
645.0	0.6	1.1	0.6	C	2888/2245	(387), 2245
648.0	1.0	1.4	0.5	C	2199/1552	722, (742), (1082), 1552
656.66	0.35	1.6	0.4		2133/1476	(313), (1448), 1476
663.44	0.32	1.8	0.3		2439/1776	(603), (1262), 1554, 1748
666.83	0.19	3.2	0.3	M		
		1.2	0.5		1257/590	456
		2.0	0.6		2088/1422	1287
677.0	0.4	2.0	0.5		1776/1099	1099
681.6	0.5	1.1	0.3		Not placed	(831), (1718)

TABLE II. (*Continued*)

Energy		Intensity			Placement from/to	Coincidences observed in this gate and remarks
688.7	0.6	1.1	0.4	C	1210/521	387
696.3	0.6	0.8	0.4	C	1776/1080	(480), (768), 931, (1080)
						1077-699 coincidence in Ag
722.25	0.12	15.6	0.7	M		
721.1	0.4	7.0	2.6		1311/590	563, 961, 1089, 1668
722.0	0.6	1.5	0.6		2273/1552	
723.1	0.4	7.1	3.2		2199/1476	511, 1448, 1476
735.83	0.21	3.1	0.1	M		
734.4	0.4	1.7	0.8		2439/1705	(625), (1705)
736.4	0.4	0.5	0.2		1257/521	387
737.5	0.4	0.9	0.3		2199/1461	1461
739.91	0.32	1.8	0.2		2708/1968	No coincidences seen
749.83	0.21	2.6	0.3		2707/1958	
782.0	0.4	1.0	0.3		2662/1880	
789.71	0.21	1.2	0.3		Not placed	
799.67	0.27	2.8	0.4		2888/2088	
807.65	0.20	2.3	0.3		1907/1099	1099
815.73	0.17	4.7	0.4		2521/1705	243, (511), (625), (1080),(1114), (1571)
835.09	0.31	1.9	0.3		Not placed	
840.3	0.4	2.8	1.1	C	2662/1822	
859.12	0.22	2.0	0.4		1958/1099	
868.59	0.25	4.5	0.5	(M)		
866.0	0.4	2.8	0.9		2888/2022	(563), 2022
867.1	0.4	1.7	0.5		2888/2020	
871.0	0.4	1.2	0.3		1461/590	
878.27	0.26	2.5	0.4		1958/1080	1080
882.21	0.12	5.6	0.7	M		
		3.0	1.1		2439/1557	1557
		2.6	1.0		2658/1776	1748
883.1	0.5	0.8	0.2		Not placed	(387), (456)
887.46	0.33	2.0	0.4		2439/1552	
906.4	0.9	1.1	0.5		Not placed	No clear coincidences
912.7	0.7	0.6	0.4	C	2012/1099	Marginal 1099-912 coincidence
920.46	0.31	1.8	0.3		2888/1968	No clear coincidences
924.7	0.7	1.0	0.5		2401/1476	(530), 1448, (1476)
931.5	0.15	4.2	0.4		2707/1776	696, (1080), 1748
939.61	0.17	4.7	0.4	(M)		
939.3	0.5	2.0	0.4		2401/1461	1461
940.4	0.5	3.0	0.6		1461/521	(387)
949.09	0.17	3.7	0.4		1083/134	1005
962.79	0.09	19.8	0.6	M		
961.6	0.6	2.5	0.9		2273/1311	(511), 563, 721, (1284), 1311
963.1	0.4	14.2	5.7		2439/1476	(511), 1448, 1476
982.08	0.35	1.8	0.4		2862/1880	
987.9	0.6	1.8	0.5		2888/1901	
1005.6	0.4	2.2	0.3		2088/1083	(562), 949
1009.4	0.5	2.3	0.3		2088/1080	1052, 1080
1023.7	0.6	1.0	0.4		2485/1461	
1034.87	0.22	2.1	0.4		2586/1552	
1045.40	0.18	2.1	0.4		2597/1552	(1552)
1052.51	0.19	7.1	1.1		1080/27	(511), 625, (1009), 1359, (1441), (1808)
1068.4	1.1	1.8	0.9	C	2161/1099	
1071.76	0.18	4.7	0.4		1099/27	No clear coincidences
1079.90	0.07	46.5	1.2		1080/0	(215), (222), (282), (464), 477, 511, 525, (668), 696, 878, 1009, (1087), (1118), (1208), 1359, 1441, (1518), (1628), 1808
1089.10	0.10	7.8	0.4	M		
1087.2	1.0	2.0	0.7		2167/1080	1080

TABLE II. (Continued)

Energy		Intensity			Placement from/to	Coincidences observed in this gate and remarks
1089.4	0.4	5.8	1.2		2401/1311	563, 721, 1311
1099.32	0.07	14.3	0.5		1099/0	(377), 558, 677, (722), 808, (859), 1301
1114.51	0.19	4.5	0.5		1705/590	456, 511, (725)
1158.0	0.8	1.0	0.5		2980/1822	Marginal 1822-1158 coincidence
1184.10	0.28	3.3	0.5		1705/521	(280), 387, 511 Ag peak at 1182.7
1209.15	0.41	1.5	0.4	(M)		
1208.2	0.6	1.9	0.7		2287/1080 (1210/0)	Not shown
1246.6	0.4	1.6	0.9	C	2707/1461 2708/1461	
1284.1	1.1	2.0	1.1	C	1311/27	
1287.61	0.10	14.3	0.7		1422/134	(424), (511), 546, (553), (563), 599, 667, (852)
1303.37	0.17	4.1	0.4	M		
1301.7	0.5	3.2	1.4		2401/1099	1099
1307.2	0.5	0.9	0.5		1828/521	370, (387)
1311.66	0.07	15.5	0.6		1311/0	(551), 961, 1089, (1275), 1668
1359.41	0.16	4.6	0.4	M		
1359.0	0.5	2.1	0.7		2439/1080	(1052), 1080
1360.2	0.4	2.5	0.9		2822/1461	1461
1379.41	0.32	2.6	0.4	M		
1377.1	0.5	1.2	0.3		1968/590 Not placed Not assigned	456, (511), (853), (920), (1074) (303), (323)
1412.83	0.17	2.9	0.4		2888/1476	1448, (1476)
1420.8	1.4	0.7	0.5	C	2012/590	Marginal 563-1420 coincidence
1428.7	0.4	3.2	0.3		2980/1552	
1434.0	0.4	2.5	0.3		1461/27	
1441.24	0.15	4.3	0.4		2521/1080	563, (1052), 1080
1448.72	0.09	53.4	1.4	M		
1447.1	0.5	6.0	1.2		1968/521	387, (511)
1448.7	0.1	47.4	1.8		1476/27	(27), 511, 724, 925, 963, 1412, 1529, (1566)
1461.81	0.07	100			1461/0	243, 496, 511, (552), 627, 737, (815), 939, (1023), (1120), (1246), 1266, (1314), 1360, (1428)
1476.27	0.11	18.3	0.8		1476/0	511, 658, 724, (925), 963, (1412), (1529)
1499.15	0.26	2.2	0.3		2020/521	
1518.0	0.5	1.4	0.3		2597/1080	
1529.29	0.17	4.9	0.5	(M)	3005/1476 (1557/27)	(563), 1448, (1476)
1552.00	0.15	23.0	0.9		1552/0	511, 648, (695), 722, (1023), 1035, (1269), 1428, 1636
1556.94	0.14	21.5	0.9		1557/0	264, 464, 511, 532, (576), 643, (736), (867), 882, (1150)
1570.15	0.15	10.1	0.8	M		
1567.5	0.5	3.0	1.1		2088/521	387
1570.6	0.5	7	4		1705/134	494, 511, (543), (815)
1573.7	0.5				Not placed	563
1627.9	0.5	1.2	0.3		2707/1080	(530), (1080)
1637.65	0.35	1.7	0.3	D		
1636.4	0.8	1.9	0.7	C	3188/1552	
1646.4	0.4	1.2	0.3		Not placed	
1659.60	0.22	2.4	0.3	DE		Double escape of 2681, no coincidences
1668.84	0.25	1.9	0.3		2980/1311	563, (721), 1311
1677.8	0.6	1.3	0.4		2199/521	
1685.22	0.39	1.4	0.4		2206/521	
1693.22	0.19	5.2	0.5	M		

TABLE II. (Continued)

Energy		Intensity			Placement from/to	Coincidences observed in this gate and remarks
					Not placed	
1694.2	0.4	1.3	0.6		1828/134	370, (1060)
1704.98	0.13	4.3	0.4		1705/0	511, (734), 815
1718.65	0.15	3.6	0.3		Not placed	681
1748.45	0.10	12.4	0.7		1776/27	(341), 511, (525), 663, 282, 931
1756.35	0.34	1.4	0.3		2855/1099	
1766.64	0.13	5.4	0.4		1901/134	188, 296, (387), (511), (825), 987
1775.79	0.21	2.3	0.3		1776/0	511
1808.74	0.21	2.9	0.3		2888/1080	
1822.02	0.11	9.0	0.5		1822/0	511, (580), 840, (1558)
1834.18	0.11	8.3	0.5		1968/134	(511), 552
1856.67	0.17	4.3	0.4		1856/0	(501), 544, (997)
1879.96	0.09	28.4	0.9	(M)		
					1880/0	318, 511, (520), 982
					(1907/27)	
					Not assigned	(615), (642), (1099)
1907.5	0.8	1.4	0.6		1907/0	
1919.00	0.18	3.5	0.4		2440/521	
1930.23	0.11	16.3	0.7		1958/27	511, (750)
1956.97	0.25	4.4	0.5	M		No coincidences
1955.9	0.5	1.7	0.2		Not placed	
1958.5	0.5	2.5	0.2		1958/0	
1972.8	0.5	1.1	0.3			Sum 511 + 1461
1984.67	0.14	4.9	0.4	(M)		No coincidences
					(1984/0)	From a (1287-563) coincidence
					(2012/27)	
1999.0	0.7	1.5	0.5	C	2521/521	
2011.95	0.11	10.9	0.5		2012/0	511, (649)
2022.53	0.13	8.7	0.5		2022/0	(511), 866
2064.63	0.35	3.0	0.4		2199/134	
2067.9	0.7	0.9	0.3	C	2658/590	456
2097.34	0.23	2.7	0.4		2125/27	No coincidences
2117.6	0.6	1.0	0.3		(2708/590)	Energy sum fitting only
2125.5	0.4	2.2	0.3		2125/0	
2133.03	0.20	16.7	0.9		2133/0	(511)
2167.66	0.25	2.5	0.3		2167/0	
2199.45	0.14	12.5	0.6		2199/0	(511)
2245.12	0.16	9.5	0.5	(M)		
					2245/0	(645)
					(2273/27)	
2257.1	0.6	1.0	0.3		2777/521	
2273.80	0.17	6.5	0.4		2273/0	No coincidences
2287.72	0.36	1.6	0.3		2288/1080	
2300.06	0.33	3.5	0.3	M		
2298.1	1.0	0.5	0.2		2888/590	
2300.1	0.4	3.3	0.7		2821/521	
2305.8	0.8	1.3	0.2		2305/0	
2328.78	0.22	2.0	0.3		2355/27	
2355.81	0.23	3.0	0.3		2355/0	
2365.7	0.8	1.7	0.3	D		
2368.0	0.6	2.2	0.7	C	2888/521	
2373.67	0.17	13.0	0.5		2401/27	(511)
2386.66	0.19	5.5	0.4		2521/134	
2401.06	0.17	10.2	0.5		2401/0	(511)
2411.72	0.28	1.8	0.3		2439/27	
2439.58	0.21	4.5	0.3		2439/0	
2457.72	0.35	1.6	0.3		2485/27	
2485.04	0.19	5.6	0.4		2485/27	

TABLE II. (Continued)

Energy		Intensity			Placement from/to	Coincidences observed in this gate and remarks
2520.91	0.34	1.5	0.3		2521/0	
2570.44	0.23	3.8	0.3		2597/27	
2597.80	0.35	1.8	0.3		2597/0	
2630.0	0.6	0.6	0.2		2658/27	
2658.1	0.5	1.4	0.3		2658/0	
2661.99	0.26	3.4	0.3		2662/0	
2681.35	0.28	12.5	0.5		2708/27	No coincidences
2688.8	1.1	1.9	0.4		2822/134	
2707.71	0.23	8.0	0.5	(M)		
					2707/0	
					2708/0	
2753.21	0.38	0.7	0.2		2888/134	
2768.65	0.35	3.3	0.4		2795/27	
2777.7	0.5	0.7	0.2		2777/0	
2795.8	0.6	0.6	0.2		2795/0	
2811.17	0.32	1.6	0.3	R		
2829.52	0.26	6.2	0.5	(M)	Unplaced	
					2855/27	
2855.53	0.28	2.8	0.4		2855/0	
2912.8	0.5	0.5	0.2	R		
2953.18	0.35	1.4	0.3		2980/27	
2980.57	0.32	1.9	0.3		2980/0	
3043.4	0.4	1.0	0.3	R		
3056.6	0.4	1.0	0.3	R		
3066.0	0.4	1.0	0.3	R		
3161.5	0.4	1.4	0.3		3188/27	
3188.5	0.4	1.5	0.3		3188/0	
3245.0	0.5	0.8	0.3	R		

keV γ ray is masked by the strong 1287 keV in the single spectra, but clear evidence for this placement is found in its presence in the coincidence spectra of the lines feeding the 1312 keV level. Clear coincidence evidence for the weak 1071 (1099 to 27) keV transition is not found. This line is placed as a consequence of its good energy fitting and as no evidence is available for another placement. The same holds for the weak 1434 (1462 to 27) keV transition. A second group of levels is placed because of their decay to the ground and 27 keV levels and coincidence data involving at least one of the 1080, 1099, 1312, 1462, or 1476 keV levels introduced above. They are listed below; the level involved in the coincidence is in parentheses: 1776 (1080, 1099), 1958 (1080, 1099), 2012 (1099), 2401 (1099, 1312, 1462, 1476), 2439 (1080, 1476), 2485 (1462), 2598 (1080), and 2981 (1312) keV levels. High energy transitions and the γ rays of the corresponding energy minus 27 keV suggest a group of levels at 2125, 2356, 2796, and 3189 keV. Though additional coincidence evidence is not found, these

assignments are supported by the lack of any coincidence involving these high energy γ rays.

As they must decay to either the ground state, first excited state, or isomeric state, the presence of the 27 keV combination makes the above assignment the most likely. Three levels are introduced from their branching to the ground and isomeric states as well as additional coincidences, namely, the 1705 (1080, 1462), 2199 (1462, 1476), and 2521 keV (1080). Coincidences indicate two cascades 387–1184 keV and 456–1114 keV fitting the 1705 to 134 energy difference. In view of the much stronger intensities of the 387 and 456 transitions, two levels are placed at 521 and 590 keV. A cascade 722–563 keV, fitting the 1312 to 27 keV difference, suggests a level at either 590 or 749 keV. As the 563 keV γ ray is known from in-beam work[3,4] to feed the $\frac{9}{2}^+$ (27 keV) state two different levels at 590 keV are indicated. This is supported by the fact that coincidence spectra of the 456 (590 to 134) and 563 (590 to 27) keV γ rays do not show common transitions. Another group of levels is supported by a branch-
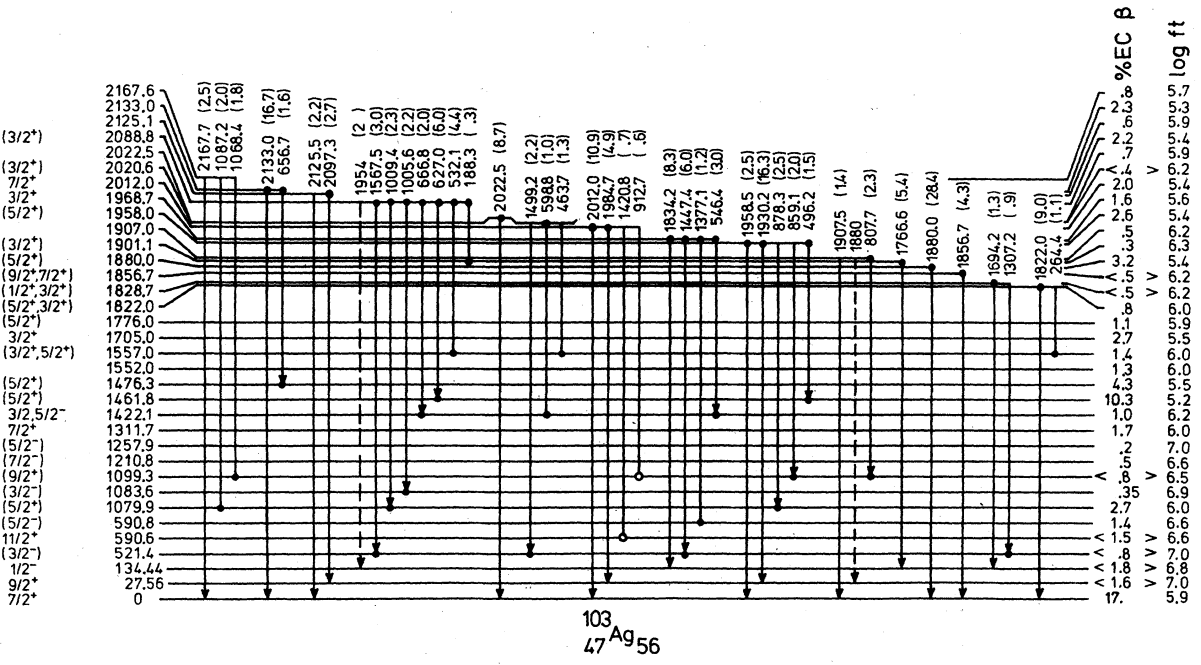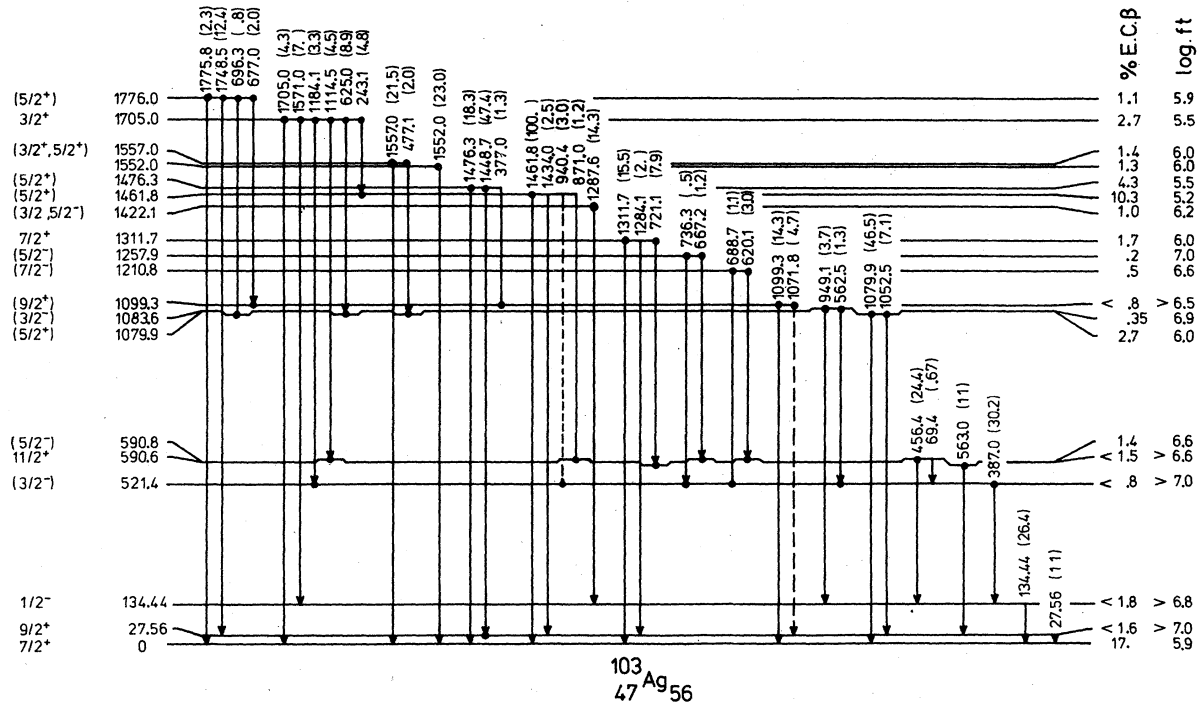
$$^{103}_{47}Ag_{56}$$

$$^{103}_{47}Ag_{56}$$

FIG. 3. Level scheme of ^{103}Ag from the decay of ^{103}Cd. Transitions with an arrow (dot) at their lower end are seen in single (coincidence) spectra. Gates were set on these transitions with a dot at their upper end. The observed coincident γ rays are listed in Table II in front of the gates. Dashed transitions are transitions with a weak evidence for the proposed placement. The γ-ray energies and intensities are given at the upper end of the transitions. Dashed transitions are not included in the intensity balances. Electron conversion has been neglected for lines other than 27 and 134 keV.

$$^{103}_{47}Ag_{56}$$

$$^{103}_{47}Ag_{56}$$

FIG. 3. (*Continued*)

TABLE III. List of levels. Assignments from selection rules are indicated without parentheses. The 27.56 keV level is regarded as uniquely assigned *a posteriori* by the $M1$ character of the 27.56 keV transition to the $\frac{7}{2}^+$ ground state and its feeding from the $\frac{11}{2}^+$ state at 590.6 keV but not from any definite $\frac{3}{2}^+$ states. Assignments in parentheses are suggested from level systematics. No assignment means only trivial assignments from selection rules are made.

Energy		J^π	β EC (%)		Log ft	Energy		J^π	β EC (%)		Log ft
0		$\frac{7}{2}^+$	17	8	5.9	2088.8	0.2	$(\frac{3}{2}^+)$	2.2	0.3	5.4
27.56	0.04	$\frac{9}{2}^+$	<1.6		>7.0	2125.1	0.3		0.6	0.1	5.9
134.44	0.05	$\frac{1}{2}^-$	<1.8		>6.8	2133.0	0.2		2.3	0.3	5.3
521.41	0.09	$(\frac{3}{2}^-)$	<0.8		>7.0	2167.6	0.3		0.8	0.2	5.7
590.6	0.4	$\frac{11}{2}^+$	<1.5		>6.6	2199.4	0.2	$\frac{3}{2}^+$	4.4	0.6	4.9
590.78	0.07	$(\frac{5}{2}^-)$	1.4	0.2	6.6	2206.6	0.4		0.18	0.05	6.4
1079.9	0.07	$(\frac{5}{2}^+)$	2.7	0.4	6.0	2245.1	0.2		1.0	0.1	5.6
1083.6	0.2	$(\frac{3}{2}^-)$	0.35	0.08	6.9	2273.7	0.2		1.3	0.2	5.4
1099.3	0.1	$(\frac{9}{2}^+)$	<0.8		>6.5	2287.8	0.4		0.4	0.1	5.9
1210.8	0.3	$(\frac{7}{2}^-)$	0.5	0.1	6.6	2356.1	0.3		0.6	0.1	5.7
1257.9	0.2	$(\frac{5}{2}^-)$	0.2	0.1	7.0	2401.0	0.1		5.6	0.6	4.7
1311.7	0.1	$\frac{7}{2}^+$	1.7	0.4	6.0	2439.4	0.1		3.8	0.8	4.9
1422.1	0.2	$\frac{3}{2},\frac{5}{2}^-$	1.0	0.2	6.2	2440.4	0.2	$\frac{3}{2}^+$	0.6	0.1	5.7
1461.8	0.1	$(\frac{5}{2}^+)$	10.3	0.9	5.2	2485.1	0.2		1.0	0.1	5.4
1476.3	0.1	$(\frac{5}{2}^+)$	4.3	0.9	5.5	2521.1	0.1	$\frac{3}{2}^+$	2.5	0.3	5.0
1552.0	0.1		1.3	0.2	6.0	2586.9	0.3		0.26	0.06	5.9
1557.0	0.1	$(\frac{3}{2}^+,\frac{5}{2}^+)$	1.4	0.2	6.0	2597.9	0.2		1.1	0.2	5.3
1705.0	0.1	$\frac{3}{2}^+$	2.7	0.7	5.5	2658.2	0.1		0.7	0.2	5.5
1776.0	0.1	$\frac{5}{2}^+$	1.1	0.2	5.9	2662.0	0.3		1.0	0.2	5.3
1822.0	0.1	$(\frac{5}{2}^+,\frac{3}{2}^+)$	0.8	0.2	6.0	2707.6	0.2		2.2	0.3	4.9
1828.7	0.4	$\frac{1}{2}^+,\frac{3}{2}^+$	<0.5		>6.2	2708.7	0.3		1.9	0.2	5.0
1856.7	0.2	$(\frac{9}{2}^+,\frac{7}{2}^+)$	<0.5		>6.2	2778.0	0.4		0.22	0.05	5.9
1880.0	0.1	$(\frac{5}{2}^+)$	3.2	0.3	5.4	2796.1	0.3		0.5	0.1	5.6
1901.1	0.2	$(\frac{3}{2}^+)$	0.3	0.1	6.3	2822.0	0.5	$\frac{3}{2}^+$	1.0	0.2	5.2
1907.0	0.2	$(\frac{5}{2}^+,\frac{7}{2}^+)$	0.5	0.1	6.2	2855.6	0.3		0.5	0.1	5.5
1958.0	0.2	$(\frac{5}{2}^+)$	2.6	0.3	5.4	2862.1	0.4		0.22	0.06	5.8
1968.7	0.2	$(\frac{3}{2}^+)$	1.6	0.3	5.6	2888.7	0.2	$\frac{3}{2}^+$	2.4	0.3	4.8
2012.0	0.1	$\frac{7}{2}^+$	2.0	0.2	5.4	2980.6	0.2		0.9	0.2	5.1
2020.6	0.3	$(\frac{3}{2}^+)$	<0.4		>6.2	3005.6	0.2		0.6	0.1	5.3
2022.5	0.2		0.7	0.1	5.9	3188.7	0.3		0.6	0.1	5.3

ing to the ground state and additional coincidences. They are, with the levels involved in coincidences in parentheses, the 1557 (1080), 1907 (1099), 2133 (1476), 2168 (1080, 1099), 2274 (1312), 2288 (1080), 2708 (1080), and 2856 (1099) keV levels. The 1211 and 1258 keV levels are based on coincidences on both the 521 and 590 (134+ 456) keV levels. A following group of levels decay to the 521 keV level. The 1084, 1829, 1969, and 2440 keV levels have, moreover, a branching to the 134 keV isomer, whereas additional coincidences support the 2021, 2089, 2778, 2822, and 2889 keV levels. The 2648 keV level is placed from

branchings to the ground and first excited states and a coincidence on the 590 (134+ 456) keV level. The next set of levels is based on their decay through a single strong γ ray and coincidence data enabling us to fit the feeding cascades into existing levels. Evidence for the 1422 keV level is found in the 522-546-1287 keV cascade. The 1552 keV level is based on the 1552 + 1428 = 2980 keV coincidence, while similarly the 1857, 1880, 2022, and 2245 keV levels are fed from the 2401 and 2889 keV levels. A few levels are introduced from a single coincidence with the intermediate level in parentheses, 2207 (521), 2587 (1552), 2862 (1880), and

3005 (1476) keV. The 1822 and 2662 keV levels decay to the ground state and to the 1557 and 1822 keV levels, respectively. Finally the 2709 keV level is based solely on energy sum fitting of three transitions to the 27, 590, and 1969 keV levels. The branching to the 590 keV (134 + 456) is assumed to be more probable from comparison with the decay patterns of other high lying levels. The occurrence of a state at 1984 keV, not reported on the level scheme, is weakly supported by the rather bad energy fitting of this transition from the 2012 to 27 keV levels and the possible existence of a 1287-563 coincidence. A last group of levels is indicated by unplaced high energy transitions. Levels must exist at the γ-ray energy or the γ-ray energy plus 27 or 134 keV as none of these γ rays are observed in coincidence spectra and their high energy and the Q_{EC} value of 4.25 MeV (Ref. 24) preclude their placement feeding into levels above 1 MeV. The corresponding γ rays are marked with an R in Table II. The unplaced intensity is not expected to change the conclusions about $\log ft$ values as it contributes only 3.7% of the decay. The single β spectra lead to a Q_{EC} value of 4.19± 0.16 MeV. The β-γ coincidence analysis, with gates set on the γ rays at 1080, 1312, 1449, 1462, 1552 + 1557, and 1880 keV, resulted in a Q_{EC} value of 4.31 ± 0.22 MeV. Both these values agree fairly well with the previous measurement by Westgaard et al.[24] of 4.25± 0.20 MeV.

V. SPIN AND PARITY ASSIGNMENTS

The β branching to the ground state has been deduced using the experimental γ-intensity balances of the excited states, the Q_{EC} value of 4.25 MeV, and the computed EC/β^+ ratios from the tables of Gove and Martin.[15] The β feedings into the 27 keV ($\frac{9}{2}^+$) and 134 keV ($\frac{1}{2}^-$) levels have been assumed to be negligible. The deduced total β^+ + EC branching to the $\frac{7}{2}^+$ ground state is (16.8 ± 7.6)%. The corresponding $\log ft$ value of 5.9± 0.2 confirms the upwards trend towards the most neutron deficient isotopes (the values in ^{105}Ag and ^{107}Ag are 5.4 and 5.0, respectively). The γ-intensity balance of the 27 keV level implies a total conversion coefficient $\alpha(27) = 12.5 \pm 2.4$. This is a lower limit as about 35 relative γ units (3.7% of the total γ intensity) have not been placed. However, taking into account some uncertainties in the level scheme and adding $\frac{1}{3}$ of the unplaced intensity to the feeding of this level, the value rises to about 18. This is the value measured in ^{105}Ag (Ref. 18) and implies a nearly pure $M1$ 27 keV transition [$\alpha(M1) = 17$, $\alpha(E2) = 160$] from Ref. 25. The deduced value from intensity balance in ^{105}Ag is higher.[19] An upper limit of 27 is obtained if

assuming all the unplaced γ intensity feeds into the 27 keV level. This corresponds to a $E2$ admixture of less than 7%. The γ-intensity balance of the 134 keV level, assuming the theoretical $\alpha(134)$ value of 3.70 (Ref. 25) for a $E3$ transition, requires an additional feeding of 17 relative γ units. This rather small value is possibly accounted for by a fraction of the unplaced intensity and also the nondetection of some weak transitions to this level. The separation of the ^{103}Ag^m (5.7 s) is not expected to be significant, considering the delay time for Ag in the ion source (~30 s) and the observation of this shortage on off-line sources. The spin and parity assignments are made on the basis of the β and γ selection rules, considering the β^+/EC allowed decay can populate only $J^\pi = \frac{3}{2}^+$, $\frac{5}{2}^+$, and $\frac{7}{2}^+$ levels and that all γ rays observed have either $E1$, $M1$, or $E2$ multipolarity (the well known isomeric $E3$ transition excepted).

A group of levels is uniquely assigned $\frac{3}{2}^+$ because of their population by allowed β decay and their branching to the $\frac{1}{2}^-$ isomer. These are the levels at 1705, 1969, 2199, 2440, 2521, 2822, and 2889 keV. The 590 keV level from 27 + 563 keV, seen in-beam has been assigned $J^\pi = \frac{11}{2}^+$ from the angular distribution of the 563 keV γ ray.[3,4] Therefore the levels at 1312 and 2012 keV, fed by allowed decay and having a branch to this $\frac{11}{2}^+$ state are uniquely assigned $\frac{7}{2}^+$ spin and parity. No other unique assignment on the basis of selection rules can be made. The levels fed by allowed β decay, with a branch to the proposed $\frac{9}{2}^+$ level at 27 keV are restricted to $J^\pi = \frac{5}{2}^+, \frac{7}{2}^+$. The levels decaying to the $\frac{1}{2}^-$ level at 134 keV are $J^\pi = \frac{3}{2}^\pm, \frac{5}{2}^-$ provided the β decay is allowed or first forbidden. These obvious considerations are not reported on the level scheme. Systematic arguments are utilized to propose spin and parity assignments for many of the low lying states. These assignments are tentative and should be regarded as an attempt to build up a systematic on basis of similarities. Such assignments are written in parentheses.

The 521 and 590 (134 + 456) keV levels have rather high $\log ft$ values which strongly suggest a forbidden β decay. The branchings to the $\frac{1}{2}^-$ level limit their spin and parity to $\frac{1}{2}$, $\frac{3}{2}$, and $\frac{5}{2}^-$. The clear systematic presence of low $\frac{3}{2}^-$ and $\frac{5}{2}^-$ states in the odd-Ag isotopes suggests the assignments of $\frac{3}{2}^-$ and $\frac{5}{2}^-$ to the 521 and 590 keV levels, respectively, as the lowest one is always the $\frac{3}{2}^-$.[19-23] The weak 69.4 keV line fitting the 590 to 521 keV difference has a branching ratio of (2.8 ±0.5)10^{-2}, similar to the corresponding one observed in ^{105}Ag (Ref. 19). The 1080 keV level is proposed as $J^\pi = \frac{5}{2}^+$ considering the occurrence of a low-lying $\frac{5}{2}^+$ state in all the odd Ag isotopes and its close resemblance to the 987 keV level in ^{105}Ag. The

1084, 1211, and 1258 keV levels have all rather
high logft values suggestive of first forbidden β
decays.

The smooth trend of the second $\frac{3}{2}^-$, $\frac{5}{2}^-$, and $\frac{7}{2}^-$
levels in the Ag isotopes suggests the assignment
$\frac{3}{2}^-$ (1084), $\frac{5}{2}^-$ (1258), and $\frac{7}{2}^-$ (1211). A possible 1211
keV transition in the 1210 multiplet may arise from
the 1211 keV level branching to the ground state.
If so, it favors the above $\frac{7}{2}^-$ assignment as a cor-
responding transition is tentatively placed in ^{105}Ag.
The 1099 keV level is not necessarily fed from al-
lowed β decay, even including the dashed 1071 keV
transition in the intensity balance. It decays to
the $\frac{7}{2}^+$ ground state and possibly the 27 keV ($\frac{9}{2}^+$)
state. An analogy with the 1097 keV in ^{105}Ag sug-
gests a $\frac{9}{2}^+$ spin and parity assignment. The 1422
keV level decays in a manner similar to the 1415
keV level in ^{105}Ag which has not been uniquely
assigned. Its branching to the $\frac{1}{2}^-$ level and the
low logft value for a forbidden transition restrict
its spin and parity to $\frac{3}{2}^+$ or $\frac{5}{2}^-$. These assign-
ments agree with its feeding only from $\frac{3}{2}^+$ or $(\frac{3}{2}^+,$
$\frac{5}{2}^+)$ levels. The level at 1462 keV is proposed as
$J^\pi = \frac{5}{2}^+$ from comparison with the 1327 keV in ^{105}Ag.
Weak evidence for a 387-940 cascade, if con-
firmed, would make this assignment unique, as-
suming one of the 521 or 590 keV levels is $\frac{3}{2}^-$.
The 1476, 1557, and 1776 keV levels have strong
branches, considering the energy dependence to
the 1080 or 1099 levels. The proposed $\frac{5}{2}^+$, $(\frac{3}{2},\frac{5}{2})^+$,
and $\frac{5}{2}^+$ spins and parities are based on analogies
with the 1441, 1386, and 1635 keV ^{105}Ag levels.
A striking correspondence exists between the
1557 and 1882 keV in ^{103}Ag with the 1386 and 1669
keV levels in ^{105}Ag. The 1822 keV level is thus
assigned $(\frac{3}{2},\frac{5}{2})^+$. The 1829 keV level decays to the
$\frac{1}{2}^-$ isomer and 521 keV, presumably $\frac{3}{2}^-$ states. It
is fed by a γ ray from the definite $\frac{3}{2}^+$ at 2199 keV
and possible forbidden β decay. The trend of the
$\frac{1}{2}^+$ states, rising up quickly with decreasing mass
number, suggests such a level in this vicinity. A
tentative $\frac{1}{2}^+$ level at 1829 keV is thus proposed as
no other neighboring level exhibits a γ deexcitation
pattern compatible with that from a $\frac{1}{2}^+$ level. Ana-
logy makes it tempting to look for a lower $\frac{1}{2}^+$ state
analog to the 1294 keV level observed in ^{105}Ag.
Assuming the cascade $\frac{1}{2}^+$ (1829) $\rightarrow \frac{1}{2}^+ \rightarrow \frac{3}{2}^-$ (521) keV,
the observation of transitions of 581 and 726 keV
in the 387 keV gate, the sum of which fits the 1829
to 521 keV energy difference, may indicate an in-
termediate level at either 1103 or 1247 keV. More
experimental evidence could not be obtained be-
cause of the limited coincidence data. Spins and
parities are proposed for the 1856 $(\frac{7}{2}^+, \frac{9}{2}^+)$, 1880
$(\frac{5}{2}^+)$, 1901 $(\frac{3}{2}^+)$, 1907 $(\frac{5}{2}^+, \frac{7}{2}^+)$, 1958 $(\frac{5}{2}^+)$, 2021 $(\frac{3}{2}^+)$,
and 2089 $(\frac{3}{2}^+)$ from more or less close resemblance
of these states to the 1718, 1750, 1635, 1886,

1986, 2156, and 2249 keV levels in ^{105}Ag. The
2089 keV assignment might be supported by a
branching to the $\frac{1}{2}^-$ level that we could not observe
due to the complex multiplet at 1955 keV.

VI. DISCUSSION

The structure of the low-energy levels in the
odd-Ag isotopes from ^{105}Ag to ^{111}Ag (Refs. 19–23)
is characterized by its smooth trend versus mass
number. The analogies on which spins and par-
ities for ^{103}Ag levels have been proposed are pos-
sible because of the continuing trend to ^{103}Ag. The
negative parity states exhibit the most regular be-
havior and have suggested two $\frac{3}{2}^-$, two $\frac{5}{2}^-$, and one
$\frac{7}{2}^-$ assignments. According to the shell model for
a nucleus with 47 protons, odd-parity states occur
from the $2p_{1/2}$- orbital and to less extent from the
$2p_{3/2}$- and $1f_{5/2}$- orbitals deeper in the shell. The
$\frac{1}{2}^-$ isomeric state may be interpreted as the $p_{1/2}$-
shell model state. The 521 $(\frac{3}{2}^-)$ and 590 $(\frac{5}{2}^-)$ keV
levels cannot be interpreted as shell model states
because of the large single particle level spacings.
These levels as well as the 1084 $(\frac{3}{2}^-)$, 1211 $(\frac{7}{2}^-)$
and 1258 $(\frac{5}{2}^-)$ are rather well accounted for by the
coupling of the single proton (hole) to the collec-
tive states of an even-even core, here ^{102}Pd (or ^{104}Cd).
The observed crossing of the $\frac{5}{2}^-$ and $\frac{7}{2}^-$ levels
between ^{107}Ag and ^{105}Ag reflects the crossing of
the 2^+_2 and 4^+ core states when considering a Pd
+ Cd average core. However, the increasing low-
ering of the $\frac{3}{2}^-, \frac{5}{2}^-$ levels relative to the core ener-
gies with decreasing mass number suggests that
the wave functions have a more complex structure
than the core-particle model predicts. Particle
transfer reaction studies indeed indicate a single
particle component in the $\frac{3}{2}^-$ states.[26–29] A more
detailed calculation using the Alaga model has
been reported by Paar.[30] The calculation has been
performed for an average $^{107-109}$Ag nucleus. Three
proton holes moving in the $2p_{3/2}$-, $2p_{1/2}$-, and $1g_{9/2}$+
orbitals are coupled to a vibrating Sn core. The
residual interaction between the extra core pro-
tons is approximated by a pairing force. The
agreement with the experiment is rather good.
The model predicts the wave function of the $\frac{1}{2}^-$
(134 keV) level to be mainly the pure shell model
orbital. The first $\frac{3}{2}^-$ and $\frac{5}{2}^-$ states still have a
main $2^+ \otimes p_{1/2}$- component, while the "two phonons"
coupled particle states are spread out over many
configurations.

It is more difficult to account for even parity
states with the core-particle coupling model.
The only single particle orbital available in the
shell is $1g_{9/2}+$. A low lying $\frac{9}{2}^+$ level and a $J^\pi = \frac{5}{2}^+$ to
$\frac{13}{2}^+$ multiplet in the 2^+ core energy region are
expected. The level at 27 keV is assigned $\frac{9}{2}^+$.

Assignments for the multiplet states have been proposed. The $\frac{5}{2}^+$ (1080 keV) and $\frac{9}{2}^+$ (1099 keV) are suggested from the systematics, whereas the $\frac{7}{2}^+$ (1312 keV) and $\frac{11}{2}^+$ (590 keV) are uniquely assigned. A $\frac{13}{2}^+$ state is found at 850 keV by in-beam study.[3,4] Thus the multiplet is widely split and its centroid lies much above the Pd or Cd core 2^+ energy. The presence of a low-lying $\frac{7}{2}^+$ level, the ground state in ^{103}Ag, near the $\frac{9}{2}^+$ single particle state is not predicted by the core plus particle model. It reveals the importance of $(g_{9/2^+})^3$ clusters. Kisslinger[31] showed that a seniority $v = 3$ j^3 coupling produces a lowering of the $I = j - 1$ state. The required quadrupole strength to reproduce the experiment was, however, unrealistically large. More recently[17] a small deformation was proposed to account for the observed isomeric $E3$ transition rate. For a prolate deformation the $\frac{7}{2}^+$ [413] Nilsson orbital is occupied by the last odd proton. Such an admixture in the wave function of the $\frac{7}{2}^+$ ground state permits the $E3$ transition to occur, as it would be forbidden if the $\frac{7}{2}^+$ state were a pure $(g_{9/2^+})^3$ coupling. A low-energy $\frac{7}{2}^+$ level is obtained by Goswami et al.[32] in the "extended quasiparticle coupling" by the coupling with backward going amplitudes. It raises the position of the $\frac{9}{2}^+$ level rather than lowering the position of the $\frac{7}{2}^+$ level so that too many low-lying levels are predicted. Further refinements including the effect of the quadrupole moment of the core[33] or an $R \cdot j$ core particle interaction[34] seem to solve this problem. Unfortunately no detailed calculation of the Ag isotopes has been presented. A new microscopic approach by Kuriyama et al.[35-37] using the "dressed quasiparticles model" is able to produce a low-lying $\frac{7}{2}^+$ level for a reasonable quadrupole strength. In this model the Pauli principle is applied between the three quasiparticles. Protons in the 28–40 shell and neutrons in the 50–82 shell are considered as core, the odd particle moves in $g_{9/2^+}$. The wave function for the $\frac{7}{2}^+$ state includes the $(g_{9/2^+})^3$ cluster as its main component plus mixtures of the $g_{9/2^+}$ orbital with various proton and neutron orbitals. The level position in ^{103}Ag is not low enough with the adopted quadrupole parameter but the trend in the Ag isotopes is reproduced though the slope is too large. The three holes core coupling calculation by Paar[30] also produced a low-energy $\frac{7}{2}^+$ state which is pushed down when switching on the particle field coupling strength. The main components of the wave function are the $(g_{9/2^+})^3$ cluster coupled to the ground state or the 2^+ phonon of the Sn core and the component expected from the simple core + particle coupling. Kuriyama and Paar present also some higher-lying positive parity states. Kuriyama et al. calculated the $\frac{5}{2}^+$, $\frac{9}{2}^+$, $\frac{11}{2}^+$, and

$\frac{13}{2}^+$ multiplet members. The trend is smooth and decreases with higher mass number. The ordering is $\frac{13}{2}^+$, $\frac{5}{2}^+$, $\frac{11}{2}^+$, and $\frac{9}{2}^+$ for the ^{101}Ag to ^{107}Ag isotopes. The experimental position of the $\frac{11}{2}^+$ and $\frac{13}{2}^+$ states at least in ^{103}Ag and ^{105}Ag is inverted. The Paar calculation reproduces as well the ordering as the quantitative energies assuming the experimental levels can be extrapolated to the $^{107-109}$Ag for which the calculation was made. The $\frac{5}{2}^+$ level is pushed up in the lightest isotopes. The slope is too low in the Kuriyama calculation. Unfortunately the Paar calculations have not been made in function of mass number to allow comparison with the experiment. Above these levels in the Paar calculation is a large gap occupied by only a $\frac{3}{2}^+$ state. No experimental evidence of a $\frac{3}{2}^+$ low-lying level is found in the lightest Ag isotopes.

A set of levels from $J = \frac{5}{2}^+$ to $\frac{17}{2}^+$ follows the gap. The $\frac{7}{2}^+$ state seems to move smoothly with mass number. A comparison with an in-beam measurement by Svensson et al.[38] locates it at 1281 keV in ^{105}Ag. Extrapolating the trend towards $^{107-109}$Ag suggests the prediction of Paar is too high. Assuming also a smooth trend for the $\frac{9}{2}^+$ state, the $\frac{9}{2}^+$ level is well reproduced by Paar. Kuriyama also calculated an almost flat behavior of the $\frac{9}{2}^+$ level in agreement with the ^{103}Ag and ^{105}Ag assignments. It seems thus that the three holes core coupling model is successful in reproducing the in first order $2^+ \otimes g_{9/2^+}$ multiplet levels. The dressed quasiparticle model on the other hand is able to reproduce the trend as function of mass number but quantitatively fails to reproduce the level positions.

Alaga and Paar[39] have shown that coupling a particle (or hole) to an anharmonic vibrator generates a band structure. They calculated the levels from the coupling of the odd particle j to the phonon of the core. The ordering and the spacing of the levels $j + 1$, $j + 2$, $j - 2$, and $j - 1$ is surprisingly close to the observed structure in ^{103}Ag for $j = \frac{9}{2}^+$ and using a particle core coupling strength of ~0.7 [see Fig. 2(a) in that paper]. Other levels have been observed which are given a different interpretation.

The $\frac{1}{2}^+$ states rise up quickly from ^{111}Ag down to ^{105}Ag. It has been suggested that this state is a particle hole state.[22,23] A weak deformation brings down the $\frac{1}{2}^+$ [431] Nilsson orbital which becomes occupied by the last odd proton. A Coriolis decoupled band built on it has been suggested in ^{111}Ag. Recent calculations by Heyde et al.[40] in the In isotopes account for this band structure with either a band mixing calculation or a superposition of two decoupled bands built on the Sn core coupling with the $2d_{5/2^+}$ and $1g_{7/2^+}$ proton orbitals. A $\frac{1}{2}^+$ level is proposed at 1829 keV in ^{103}Ag as it is the only observed level consistent with this assign-

ment. The $(^3\mathrm{He},d)$ transfer reaction[26] shows the increasing fragmentation of the $\frac{3}{2}^+$ and possibly $\frac{5}{2}^+$ particle hole states towards $^{103}\mathrm{Ag}$, so that assignments for other band members are difficult.

In $^{105}\mathrm{Ag}$ Jackson et al.[19] remarked the tendency for logft values to the high excited states to become close to the logft value for a Gamow-Teller decay of $g_{9/2^+}$ to $g_{7/2^+}$. The Q_{EC} value of $^{103}\mathrm{Cd}$ decay, higher than for $^{105}\mathrm{Cd}$ decay, allows the observation of more of such states. The final $^{103}\mathrm{Ag}$ levels are interpreted as $\pi\nu^2$ states implying neutron excitations of the core. Such particle excitations in $^{104}\mathrm{Pd}$ have been suggested.[41,42] An explanation for the numerous high-energy transitions feeding into the ground $\frac{7}{2}^+$ or first excited $\frac{9}{2}^+$ states is to regard these as collective effects implying neutron transitions. The three-hole core coupling model is not at present able to deal with $\pi\nu^2$ states. However, the "dressed quasiparticle" model treats protons and neutrons on equal footing. It would be of great interest to obtain detailed calculations of levels in this energy region with this model. It is worth noting that the gross distribution of the β branchings in the $^{105}\mathrm{Cd}$ and $^{103}\mathrm{Cd}$ decays is quite similar, but that the logft values in $^{103}\mathrm{Cd}$ decay seem systematically higher than in $^{105}\mathrm{Cd}$ decay, by a factor of about 0.5. This reflects a general retardation of the β decay process when removing two neutrons. An explanation for it has not yet been found. This behavior differs from the trend of the Pd isotopes,[43-45] which have only two protons less.

VII. CONCLUSION

The low-energy level structure of the odd-mass Ag isotopes is now known between $A = 103$ and $A = 111$. The need for models other than the simple core + particle coupling is clearly established by the presence of the low-lying $\frac{7}{2}^+$ state and the large splitting of the $\frac{5}{2}^+$ to $\frac{13}{2}^+$ multiplet. The calculations with the "dressed" quasiparticles or the three-hole vibration coupling seem to account at least qualitatively for the observed structure. However, specific calculations for each isotope have not been reported and it would be interesting to compare the predictions of these models with the data now available.

ACKNOWLEDGMENTS

*Aspirant N.F.W.O.

[1]P. G. Hansen et al., Phys. Lett. 28B, 415 (1969).

[2]I. L. Preiss, P. J. Estrup, and R. Wolfgang, Nucl. Phys. 18, 624 (1960).

[3]J. Ludziejewski, J. Bron, W. H. A. Hesselink, A. W. B. Kalshoven, A. van Poelgeest, H. Verheul, R. Kamermans, and M. J. A. de Voigt, in Proceedings of the International Conference on Nuclear Physics, 1977 (unpublished).

[4]R. Béraud, A. Charvet, R. Duffait, J. Genevey-Rivier, J. Letessier, M. Meyer, and J. Tréherne, in Proceedings of the International Conference on Nuclear Physics, Tokyo, Japan, 1977 (unpublished).

[5]W. White and W. M. Martin, Can. J. Phys. 40, 865 (1962).

[6]W. Dietrich, B. Nyman, A. Johansson, and A. Bäcklin, Phys. Scri. 12, 80 (1974).

[7]G. Dumont et al., Nucl. Instrum. Methods 153, 81 (1978).

[8]M. Blann and F. Plasil, Phys. Rev. C 11, 508 (1975).

[9]M. Blann and F. Plasil, Nuclear Research Laboratory, Univ. of Rochester, Report No. COO-3494-29, 1976 (unpublished).

[10]J. Van Klinken, S. J. Feenstra, K. Wisshak, and H. Faust, Nucl. Instrum. Methods 130, 427 (1975).

[11]J. De Raedt, Nucl. Instrum. Methods 108, 333 (1973).

[12]P. C. Simms, Purdue University Accelerator Laboratory, West Lafayette, Indiana 47907, private communication.

[13]A. H. Wapstra and N. B. Gove, Nucl. Data A9, 267 (1971).

[14]S. Maripuu, Nucl. Data A17, 477 (1976).

[15]N. B. Gove and M. J. Martin, Nucl. Data Tables 10, 205 (1971).

[16]W. B. Ewbank, L. L. Marino, W. A. Nierenberg, H. A. Shugart, and H. B. Silbee, Bull. Am. Phys. Soc. 3, 370 (1958).

[17]V. R. Casella, J. D. Knight, and R. A. Nauman, Nucl. Phys. A239, 83 (1975).

[18]L. G. Svensson, O. Bergman, A. Bäcklin, N. G. Jonsson, and J. Lindskog, Phys. Scri. 14, 129 (1976).

[19]S. V. Jackson, W. B. Walters, and R. A. Meyer, Phys. Rev. C 13, 803 (1976).

[20]T. Paradellis and C. A. Kalfas, Z. Phys. 271, 79 (1974).

[21]G. Berzins, M. E. Bunker, and J. W. Starner, Nucl. Phys. A126, 273 (1969).

[22]G. Berzins, M. E. Bunker, and J. W. Starner Nucl. Phys. A114, 512 (1968).

[23]W. C. Schick Jr. and W. L. Talbert Jr., Nucl. Phys. A128, 353 (1969).

[24]The ISOLDE collaboration L. Westgaard et al., in Proceedings of the 4th International Conference on Atomic Masses and Fundamental Constants, Teddington, Eng-

land,1971, edited by J. H. Sanders, A. H. Wapstra, Eds, (Plenum, New York, 1972).

[25]R. S. Hager and E. C. Seltzer, Nucl. Data A4, 1 (1968).

[26]R. E. Anderson and J. J. Kraushaar, Nucl. Phys. A241, 189 (1975).

[27]R. E. Anderson, R. L. Bunting, J. D. Burch, S. R. Chinn, J. J. Kraushaar, R. J. Peterson, D. E. Prull, B. W. Ridley, and R. A. Ristinen, Nucl. Phys. A242, 75 (1975).

[28]R. L. Auble, F. E. Bertrand, Y. A. Ellis, and D. J. Horen, Phys. Rev. C 8, 2308 (1973).

[29]S. Y. Van Der Werf, B. Fryszczyn, L. W. Put, and R. H. Siemssen, Nucl. Phys. A273, 15 (1976).

[30]V. Paar, Nucl. Phys. A211, 29 (1973).

[31]L. S. Kisslinger, Nucl. Phys. 78, 341 (1966).

[32]A. Goswami and A. I. Sherwood, Phys. Rev. 4, 1232 (1967).

[33]A. Goswami and O. Nalcioglu, Phys. Lett. 26B, 353 (1968).

[34]A. Goswami, D. K. Mc Daniels, and O. Nalcioglu, Phys. Rev. C 7, 1263 (1973).

[35]A. Kuriyama, T. Marumori, and K. Matsuyanagi, Prog.

Theor. Phys. 47, 498 (1972).

[36]A. Kuriyama, T. Marumori, and K. Matsuyanagi, Prog. Theor. Phys. 51, 779 (1974).

[37]A. Kuriyama, T. Marumori, and K. Matsuyanagi, Prog. Theor. Phys. Suppl. 58, 53 (1975).

[38]L. G. Svensson, N. G. Jonsson, and J. Linkskog UUIP Uppsala University, Institute of Physics, Progress Report No. 6.1.8, 1975 (unpublished).

[39]G. Alaga and V. Paar, Phys. Lett. 61B, 129 (1976).

[40]K. Heyde, M. Waroquier, P. Van Isacker, and H. Vincx, Nucl. Phys. A292, 237 (1977).

[41]N. C. Singhal, N. R. Johnson, E. Eichler, and J. H. Hamilton, Phys. Rev. C 5, 948 (1972).

[42]K. Okano, Y. Kawase, and S. Uehara, Nucl. Phys. A182, 131 (1972).

[43]M. E. Phelps, D. G. Sarantites, Nucl. Phys. A135, 116 (1969).

[44]M. E. Phelps, D. G. Sarantites, Nucl. Phys. A159, 113 (1970).

[45]W. H. Zoller, E. S. Macias, M. T. Perkal, and W. B. Walters, Nucl. Phys. A130, 293 (1969).